Supporting Information

Self-assembly synthesis of CuSe@graphene-carbon nanotubes as efficient and robust oxygen reduction electrocatalyst for microbial fuel cells

Liang Tan, Nan Li*, Shuang Chen, Zhao-Qing Liu*

School of Chemistry and Chemical Engineering/Guangzhou Key Laboratory for Environmentally Functional Materials and Technology Guangzhou University; Guangzhou Higher Education Mega Center, Waihuan Xi Road No. 230, China 510006
Fax: 86-20-39366908; Tel: 86-20-39366908;
**E-mail: nanli@gzhu.edu.cn (N. Li); lzqgzu@gzhu.edu.cn (Z. Q. Liu)*

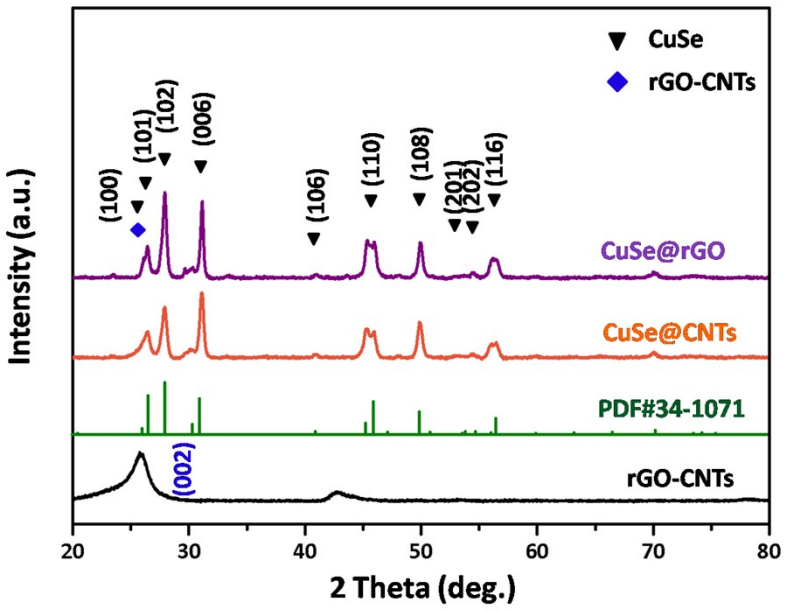

Fig. S1 XRD patterns of the CuSe@rGO-CNTs, CuSe@rGO and CuSe@CNTs composites.

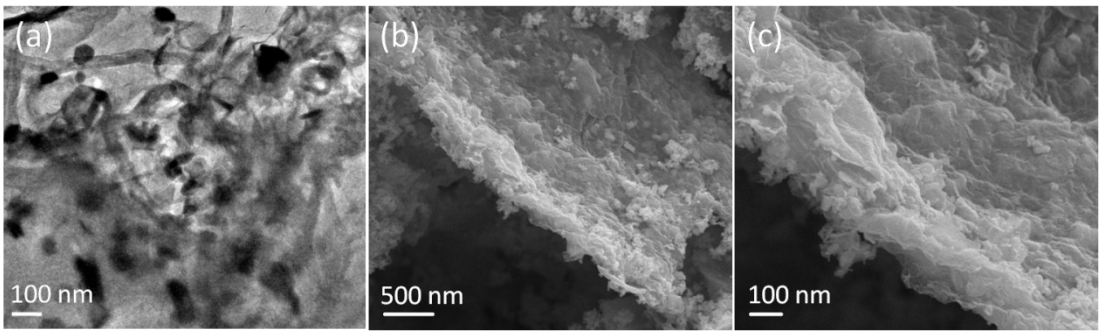

Fig. S2 (a,b) The SEM imges of CuSe@rGO/CNTs in the different magnification; (c) The TEM imges of CuSe@rGO-CNTs composite.

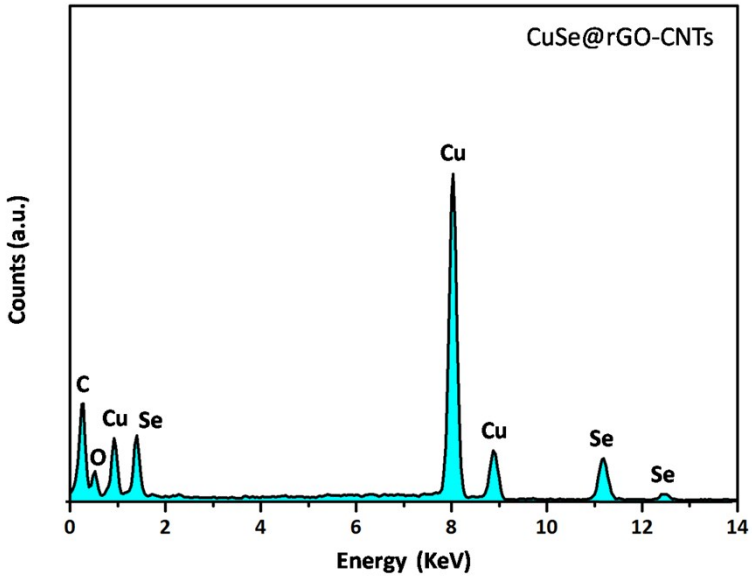

Fig. S3 EDS spectra of the CuSe@rGO-CNTs compound.

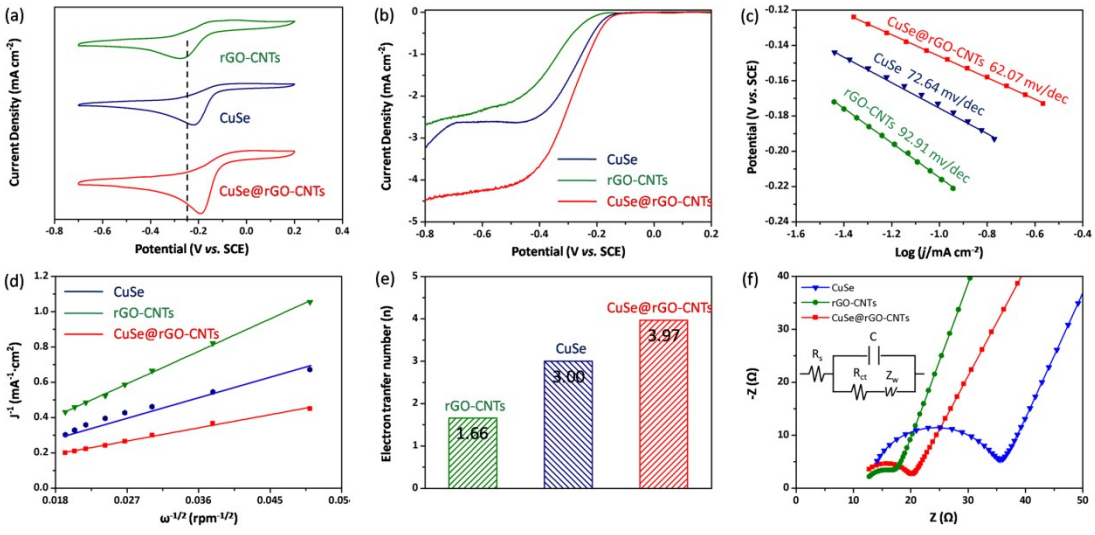

Fig. S4 (a) CV curve of different catalysts in saturated Oxygen at the scan rate of 10 mV s^{-1}; (b) LSV curve of different catalysts in 0.1 M KOH solution at the scan rate of 5 mV s^{-1} with 1700 rpm; (c) Tafel curve; (d) K-L curve; (e) electron transfer number; (f) Nyquist curve of rGO/CNTs, CuSe and CuSe@rGO-CNTs, and inserted fitting circuit for Nyquist curve.

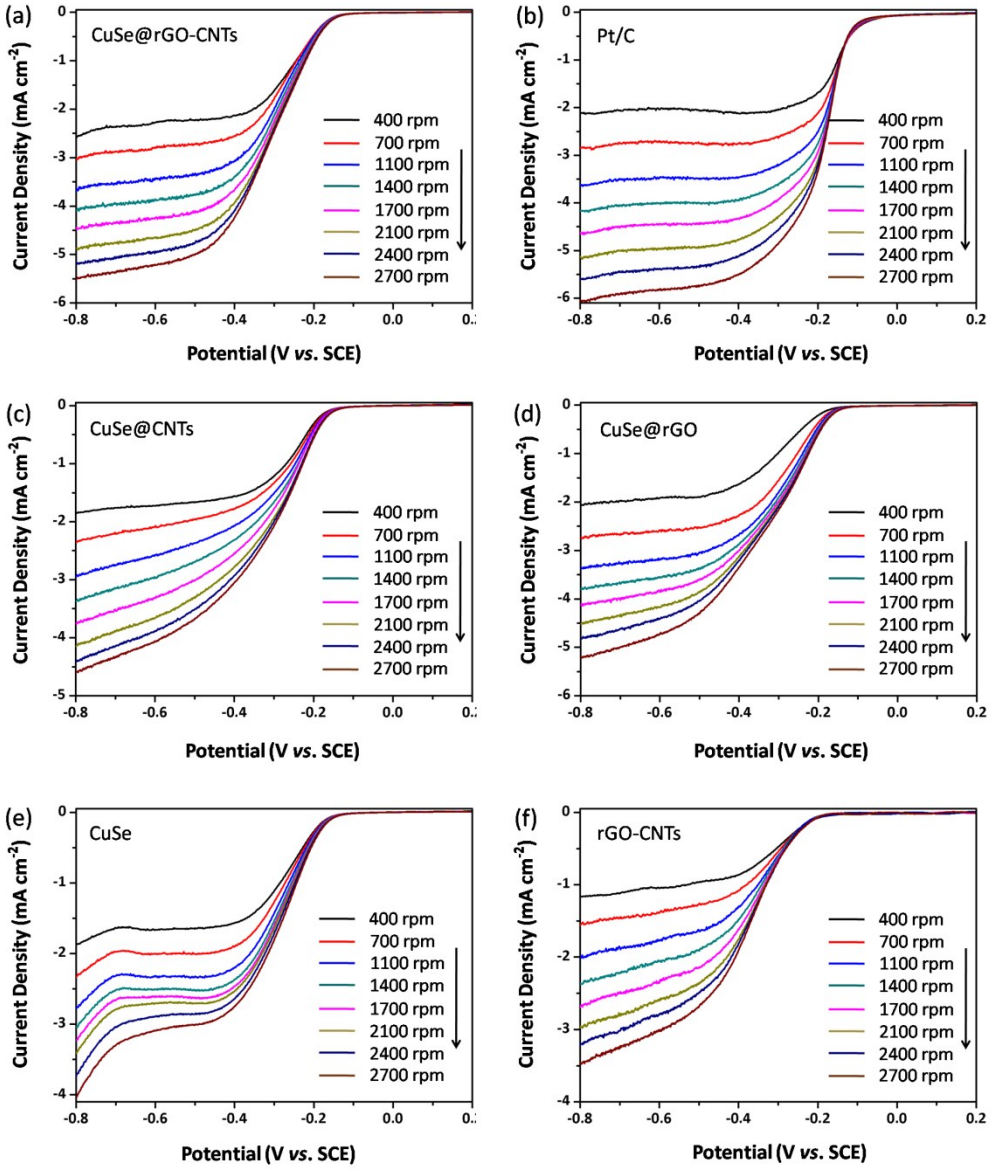

Fig. S5 Rotating disk electrode test of catalyst with (a) CuSe, (b) CuSe@CNTs, (c) CuSe@rGO, (d) rGO-CNTs, (e) CuSe@rGO-CNTs and (f) Pt/C at 400-2700 rpm.

Table. S1 The main parameter from Nyquist curve.

para	Pt/C	CuSe@rGO-CNTs	CuSe@rGO	CuSe@CNTs	CuSe	rGO-CNTs
R_s	11.58	11.02	10.78	9.61	12.84	11.88
R_{ct}	5.092	8.56	16.88	18.79	21.78	4.96

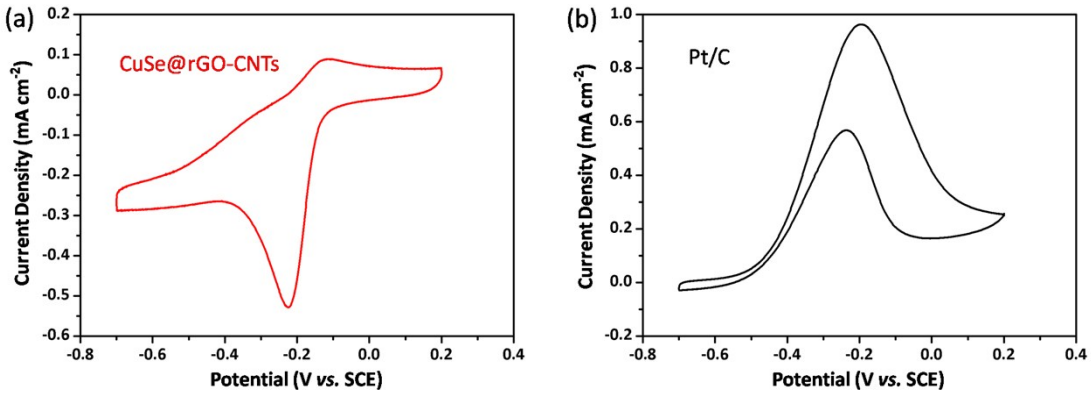

Fig. S6 (a-b) CV curves of CuSe@rGO-CNTs and Pt/C electrodes were recorded in the presence of methanol.

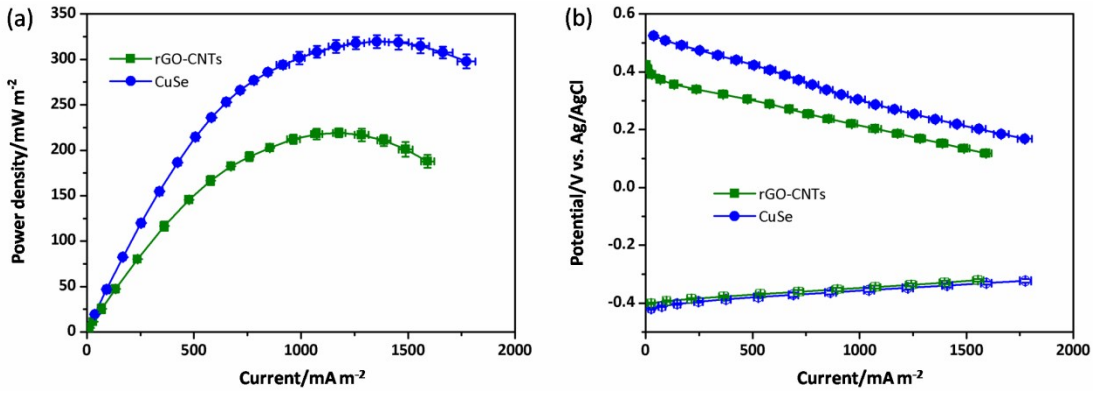

Fig. S7 (a) Power density curves; (b) Entire cells and anode (vs. Ag/AgCl) polarization curves for different catalyst materials.

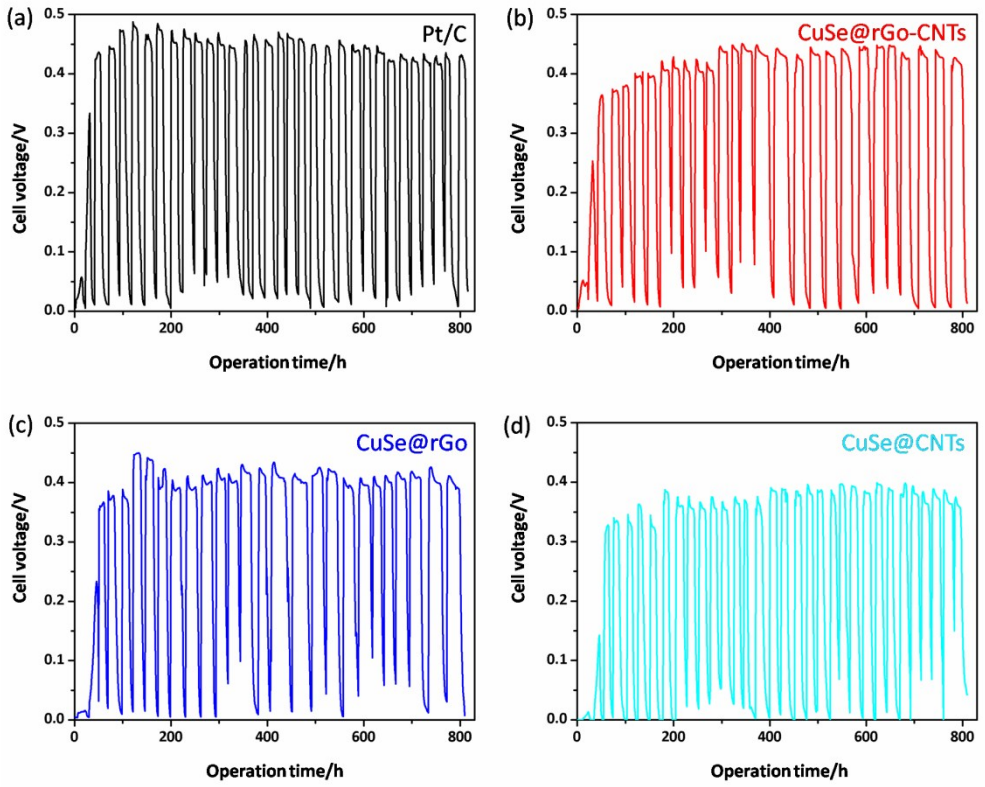

Fig. S8 (a-d) The voltage-time profile of MFCs with different cathode catalysts.

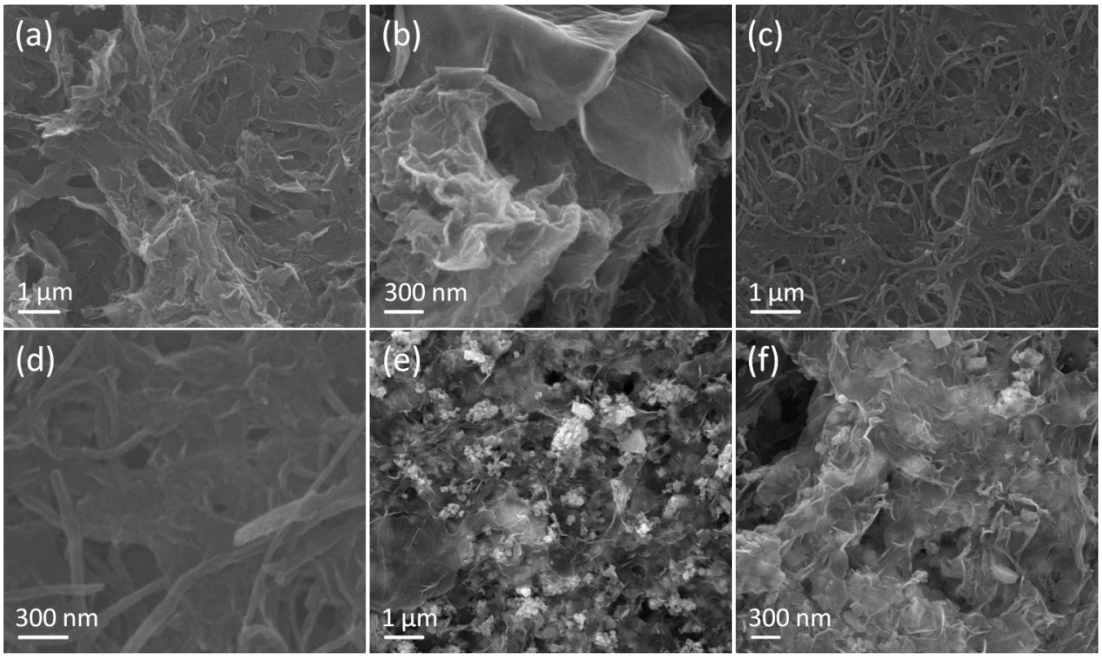

Fig. S9 (a, b) SEM imges of GO in the different magnification; (c, d) SEM imges of rGO-CNTs in the different magnification; (e, f) SEM imges of CuSe@rGO in the different magnification.

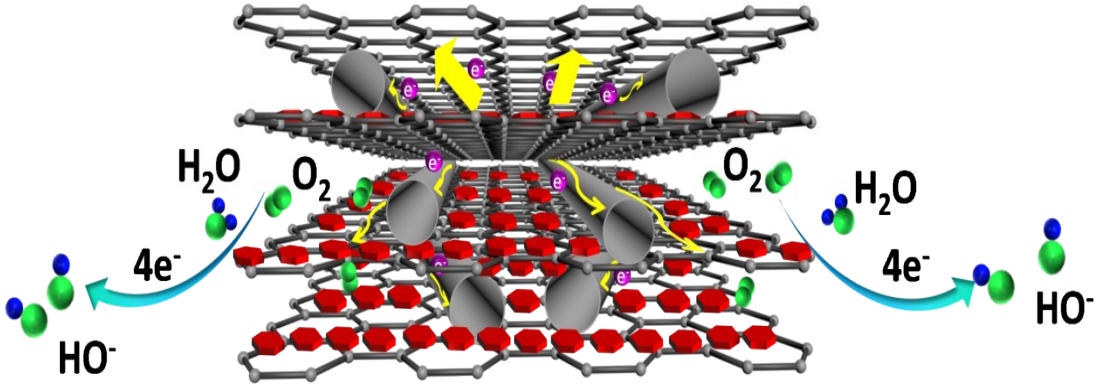

Fig. S10 The schematic illustration of electron transfer process in ORR.

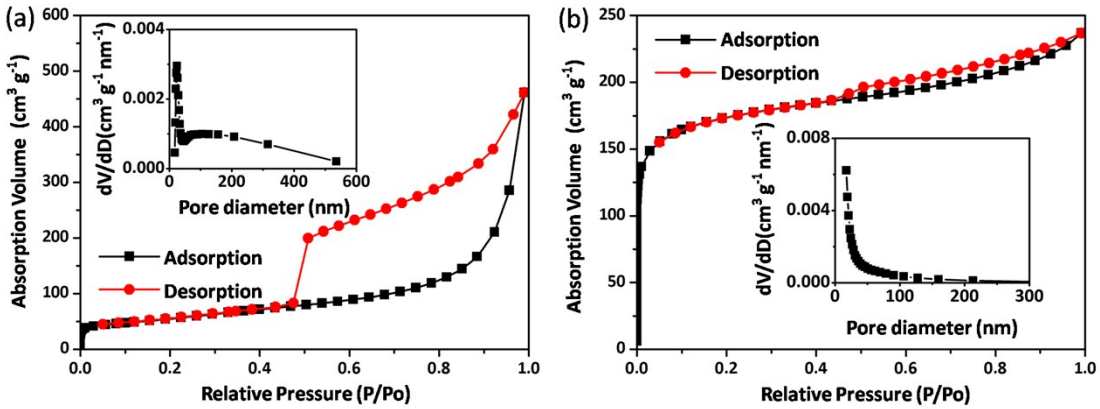

Fig. S11. N_2 isothermal adsorption of (a) CuSe@rGO-CNTs and (b) Pt/C, and the inset are the corresponding pore distribution.

As seen in **Fig. S11a**, the as-prepared CuSe@rGO-CNTs sample possesses a high BET (Brunauer-Emmett-Teller) specific surface area of 197.45 m^2 g^{-1} and a pore volume of 0.49 cm^3 g^{-1}. The pore size distribution of CuSe@rGO-CNTs determined from nitrogen adsorption isotherm shows the presence of mesopores and macropore from ~26 to 500 nm. Such superior specific surface area clearly higher than these already reported hybrid materials of graphene supported metal composite. (For examples, Mn_3O_4/NG, Adv. Funct. Mater., 2014, 24, 2072-2078; Fe/N-gCB, Chem. Commun, 2015, 51, 7516-7519; $FeCo_2O_4$/HrGOS, Carbon, 2015, 92, 74-83; Fe_3O_4/N-GAs, J. Am. Chem. Soc, 2012, 134, 9082-9085.) Moreover, the commercial Pt/C hold the BET specific surface are of 496.86 m^2 g^{-1} and a pore volume of 0.37 cm^3 g^{-1}. (**Fig. S11b**)

The MFCs performance is difficult to compare directly with other literatures since the different adopted parameters, such as the organic substrate, buffer system, inoculated bacterial strain, cell configuration, catalyst content, etc. Herein, similar MFCs device was fabricated for better comparison by using commercial Pt/C as air cathode under the same identical configuration and operation conductions. The MFCs with the CuSe@rGO-CNTs cathode catalyst generates a maximum power density of 504 ± 5 mW m^{-2}, which is comparable to that of the Pt/C (525 ± 8 mW m^{-2}). Moreover, the CuSe@rGO-CNTs also exhibits higher catalytic effect that previously reported catalysts with identical or similar mass loading. The detailed comparison was also

shown in **Table S2.**

Table S2. The MFCs activity comparison with different cathodes

Reference	Mass loading [mg cm-2]	Maximum power density	Maximum power density of Pt/C	Percentage to Pt/C (%)
In this work	**3**	**504±5 mW m^{-2}**	**525±8 mW m^{-2}**	**96**
HP-Fe-N-C-900[1]	3	0.14±0.01 mW cm^{-2}	0.15±0.01 mW cm^{-2}	93.3
C-CoOx-CoPc[2]	6	780±39 W cm^{-2}	850±42 W cm^{-2}	91.8
$MnFe_2O_4$/NPs/Pani[3]	0.5	6.49 W m-3	6.88 W m-3	94.3
Fe-AAPyr[4]	5±0.5	59 µW cm-2	87 µW cm-2	67.8
Powered-SMs[5]	5	969±28 mWm^{-2}	1069±15 mWm^{-2}	90.6
C/ZrO_2[6]	5	596 ±3 mWm^{-2}	945 ±5 mWm^{-2}	63.1
N-S-CMK[7]	2	88.2mWcm^{-2}	105mWcm^{-2}	84
N- G/CoNi/BCNT[8]	5	2.0±0.1 W m^{-2}	2.6±0.2 W m^{-2}	76.9
Pani-MnO_2[9]	5	0.0376 W m^{-2}	0.0588 W m^{-2}	63.9
FePcMnOx/MON[10]	1.6	143 mWm^{-2}	140 mWm^{-2}	102.1

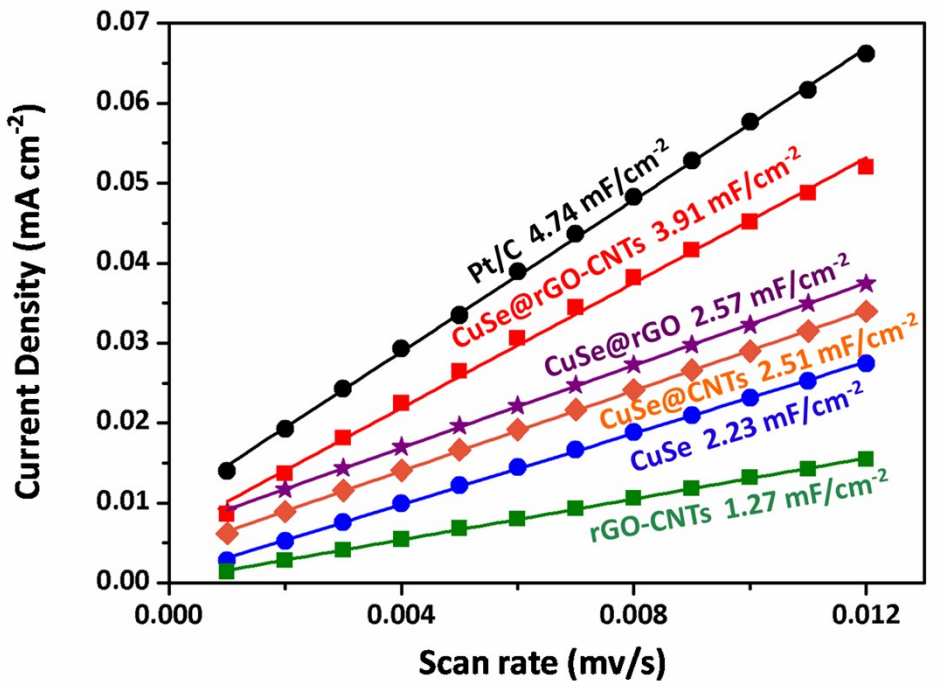

Fig. S12. Plot showing the extraction of the double layer capacitance (C_{dl}) of the different catalysts in the ORR.

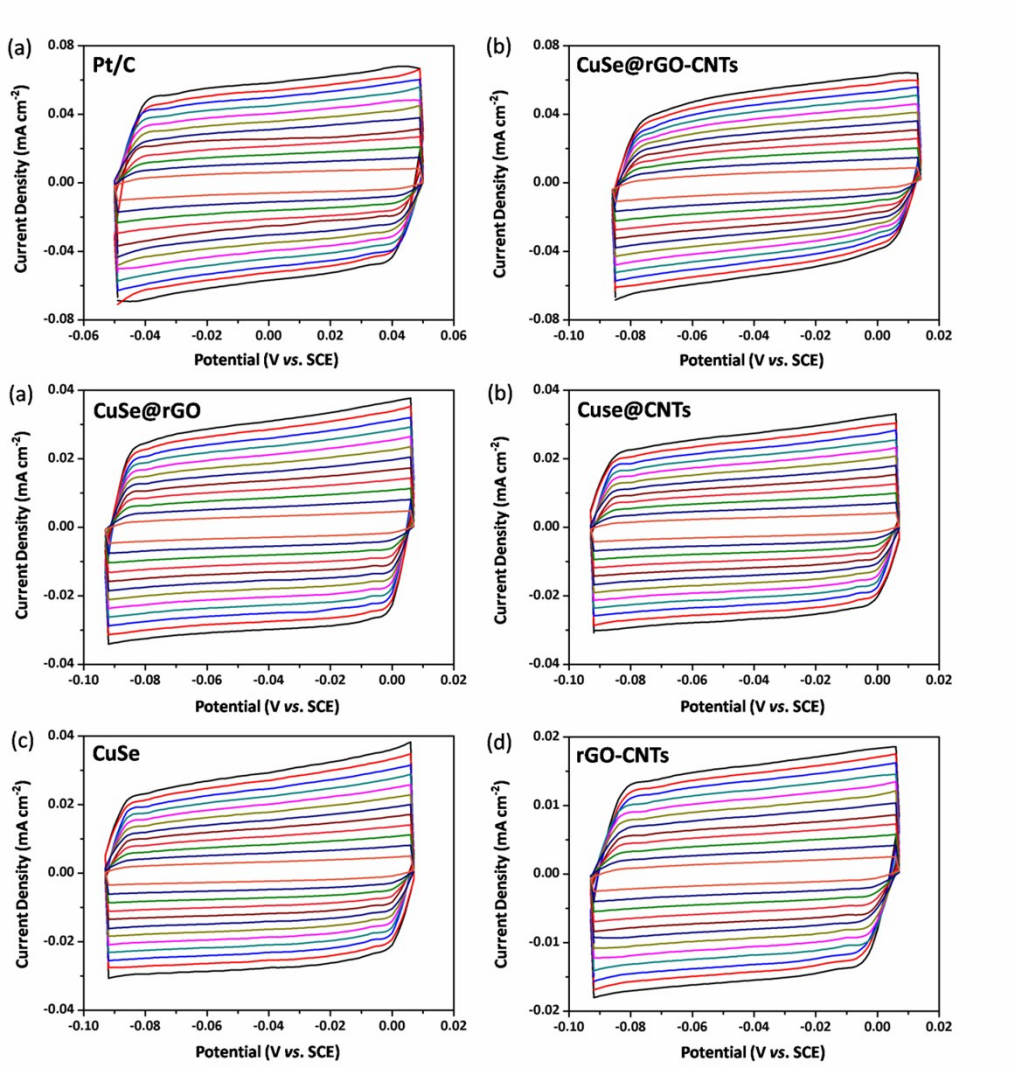

Fig. S13. Cyclic voltammograms recorded for different catalytic at various scan rates (from 12 mV/s to 1 mV/s) to determine the double layer capacitance (C_{dl}) of ORR.

We have measured the value of double-layer capacitance (C_{dl}), which is proportional to effective active surface area. [11-12] As seen in **Figure S11** and **S12**, rGO-CNTs has reveal a lower C_{dl}, indicating its poor active surface area; and the C_{dl} of pure CuSe is comparable to the value of CuSe@CNTs and CuSe@rGO, which demonstrated than CuSe could be the key active sites for the ORR. However, the superior ORR performance was largely limited by the weak conductivity and the formation of metal clusters of CuSe. Interestingly, the interconnected rGO-CNTs hybrid structure could be efficient prevent the formation of CuSe metal clusters and remedy them poor

conductivity, and also explain this reason which the high active surface area was obtained in the prepared CuSe@rGO-CNTs..

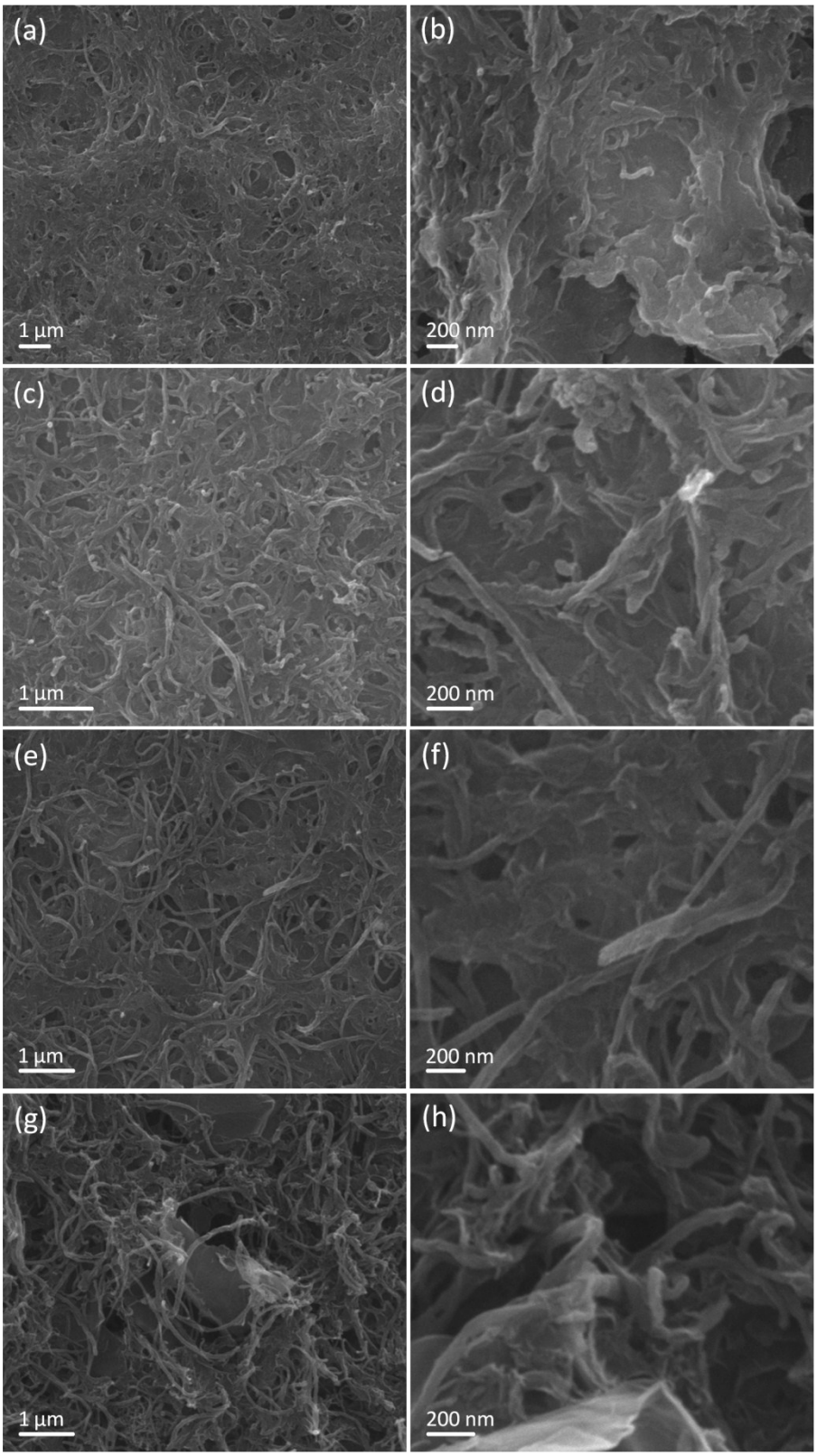

Fig. S14. SEM images of as-prepared rGO-CNTs samples from different mass ratio between

CNTs and rGO. (a-b) the mass ratio between CNTs and rGO was 1:4; (c-d) 1:3; (e-f) 1:2 and (g-h) 1:1.

To obtain the optimal content ratio of CNTs : rGO, different contents ratio of CNTs : rGO were prepared. As shown in **Figure S14**, obvious interconnected structure can be found with the increase of CNTs amount. However, lower CNTs amount can't prevent the agglomerate tendency of rGO, and excessive content of CNTs may cause the accumulation of CNTs. As a result, the optimal ratio amount should be 1:2 (CNTs: rGO).

References

[1] Y. H. Su, H. L. Jiang, Y. H. Zhu, W. J. Zou, X. L. Yang, J. D. Chen, C. Z. Li, *J. Power Sources*, 2014, 265, 246-253.

[2] J. Ahmed, H. J. Kim, S. Kim, *RSC Adv*., 2014, 4, 44065-44072.

[3] S. Khilari, S. Pandit, J. L. Varanasi, D. Das, D. Pradhan, *ACS Appl. Mater. Interfaces*, 2015, 7, 20657-20666.

[4] C. Santoro, A. Serov, C. W. N. Villarrubia, S. Stariha, A. J. Schuler, K. Artyushkova, P. Atanassov, *ChemSusChem*, 2015, 8, 828-834.

[5] Y. Yuan, T. Liu, P. Fu, J. H. Tang, S. G. Zhou, *J. Mater. Chem. A*, 2015, 3, 8475-8482.

[6] B. Mecheri, A. Lannaci, A DEpifanio, A. Mauei, S. Licoccia, *ChemPlusChem*, 2016, 81, 80-85.

[7] Y. Qiu, J. J. Huo, F. Jia, B. H. Shanks, W.Z. Li, *J. Mater. Chem. A*, 2016, 4, 83-95.

[8] Y. Hou, H. Y. Yuan, Z. H. Wen, S. M. Cui, X. R. Guo, Z. He, J. H. Chen, *J. Power Sources*, 2016, 307, 561-568.

[9] S. A. Ansari, N. Parveen, T. H. Han, M. O. Ansari, M. H. Cho, *Phys. Chem. Chem. Phys*., 2016, 18, 9053-9060.

[10] R. Burkitt, T. R. Whiffen, E. H. Yu, *Appl. Catal., B*, 2016, 181, 279-288.

[11] X. H. Gao, H. X. Zhang, Q. G. Li, X. G. Yu, Z. L. Hong, X. W. Zhang, C. D. Liang, Z. Lin, *Angew. Chem. Int. Ed*., 2016, 55, 6290-6294.

[12] C. C. L. McCrory, S.H. Jung, I. M. Ferrer, S. M. Chatman, J. C. Peters, T. F. Jaramillo, *J. Am. Chem. Soc*., 2015, 137, 4317-4357.